1995

The Majority of Yeast UPF1 Co-localizes with Polyribosomes in the Cytoplasm

Audrey L. Atkin
University of Nebraska-Lincoln, aatkin@unl.edu

Nicola Altamura
l'Universita di Bari

Peter Leeds
University of Wisconsin-Madison

Michael R. Culbertson
University of Wisconsin-Madison

Molecular Biology of the Cell
Vol. 6, 611–625, May 1995

The Majority of Yeast UPF1 Co-localizes with Polyribosomes in the Cytoplasm

Audrey L. Atkin,* Nicola Altamura,† Peter Leeds,*‡ and Michael R. Culbertson*§

*Laboratories of Genetics and Molecular Biology, University of Wisconsin, Madison, Wisconsin 53706; and †Centro di Studio sui Mitocondri e Metabolismo Energetico, Consiglio Nazionale delle Ricerche, presso l'Universita di Bari, Bari, 70126 Italy

Submitted December 29, 1994; Accepted March 8, 1995
Monitoring Editor: Peter Walter

In *Saccharomyces cerevisiae* the UPF1 protein is required for nonsense-mediated mRNA decay, the accelerated turnover of mRNAs containing a nonsense mutation. Several lines of evidence suggest that translation plays an important role in the mechanism of nonsense mRNA decay, including a previous report that nonsense mRNAs assemble in polyribosomes. In this study we show that UPF1 and ribosomal protein L1 co-localize in the cytoplasm and that UPF1 co-sediments with polyribosomes. To detect UPF1, three copies of the influenza hemagglutinin epitope were placed at the C-terminus. The tagged protein, UPF1–3EP, retains 86% (± 5%) of function. Using immunological detection, we found that UPF1–3EP is primarily cytoplasmic and was not detected either in the nucleus or in the mitochondrion. UPF1–3EP and L1 co-distributed with polyribosomes fractionated in a 7–47% sucrose gradient. The sucrose sedimentation profiles for UPF1–3EP and L1 exhibited similar changes using three different sets of conditions that altered the polyribosome profile. When polyribosomes were disaggregated, UPF1–3EP and L1 accumulated in fractions coincident with 80S ribosomal particles. These results suggest that UPF1–3EP associates with polyribosomes. L3 and S3 mRNAs, which code for ribosomal proteins of the 60S and 40S ribosomal subunits, respectively, were on average about 100-fold more abundant than UPF1 mRNA. Assuming that translation rates for L3, S3, and UPF1 mRNA are similar, this result suggests that there are far fewer UPF1 molecules than ribosomes per cell. Constraints imposed by the low UPF1 abundance on the functional relationships between UPF1, polyribosomes, and nonsense mRNA turnover are discussed.

INTRODUCTION

Messenger RNA abundance is determined by the relative rates of mRNA synthesis and decay. Regulation often occurs at both levels to achieve the flexibility needed for a rapid cellular response to environmental changes or developmental programs (Sachs, 1993). Although much more is currently known about transcriptional regulatory mechanisms, the general features of mRNA decay pathways are beginning to emerge.

Recently, several genes have been identified in *Saccharomyces cerevisiae* and *Caenorhabditis elegans* whose products participate in one or more pathways leading to accelerated decay of mRNAs that terminate translation prematurely because of a nonsense mutation (Leeds *et al.*, 1991, 1992; Pulak and Anderson, 1993). This kind of mRNA decay process, referred to as "nonsense-mediated mRNA decay" (Peltz and Jacobson, 1993), may serve a useful purpose by degrading mRNAs that contain a premature block in translation due to errors in transcription and processing (He *et al.*, 1993; Pulak and Anderson, 1993). Such a system

‡ Present address: McArdle Laboratory for Cancer Research, University of Wisconsin, Madison, WI 53706.
§ Corresponding author: Laboratory of Molecular Biology, R.M. Bock Building, University of Wisconsin, 1525 Linden Drive, Madison, WI 53706.

would prevent the accumulation of potentially deleterious truncated proteins. In addition, these pathways may also control the steady state levels of some specific mRNAs as suggested by Leeds *et al.* (1991).

Nonsense mRNAs appear to be targeted for accelerated decay due to premature translational termination, implying that mRNA decay pathways of this type act in concert with translation. Functional coupling of translation and nonsense mRNA decay is further suggested by the observation that efficient tRNA nonsense suppressors restore stability to nonsense mRNAs (Losson and Lacroute, 1979; Gozalbo and Holmann, 1990; Belgrader *et al.*, 1993). Hairpin structures inserted in the 5′-untranslated region of mRNA that reduce the rate of translational initiation restore stability to nonsense mRNA (Belgrader *et al.*, 1994). Also, nonsense mRNAs that are subject to accelerated decay are found to be associated with polyribosomes that are actively engaged in translation (Leeds *et al.*, 1991).

In *S. cerevisiae*, studies of the *UPF1* and *UPF3* genes have led to new insights into the mechanism of nonsense mRNA decay (Leeds *et al.*, 1991, 1992). In strains lacking a functional *UPF1* or *UPF3* product, the decay rate of nonsense mRNA is restored to a level comparable to the corresponding wild-type mRNA, but the half-life of the wild-type mRNA remains unaltered. Unlike tRNA suppressors that were shown to stabilize nonsense mRNAs by promoting translational readthrough of a premature stop codon (Losson and Lacroute, 1979), loss of *UPF1* function does not appear to enhance read-through (Leeds *et al.*, 1991). These results suggest that despite the dependence of nonsense mRNA decay on efficient premature translational termination, the *UPF1* product does not stimulate decay merely by ensuring efficient termination. Considering that *upf1*$^-$ cells are also hypersensitive to cycloheximide, an inhibitor of translational elongation, it seems likely that one or more of the *UPF* gene products will be found to interact directly with ribosomes actively engaged in translation.

Although nonsense mRNA decay may be triggered in physical proximity with cytoplasmic ribosomes, recent studies in mammals suggest that a complex mechanism is possible. Cheng and Maquat (1993) measured the accumulation of human TPI mRNA and found that nonsense mutations reduced the accumulation of both nuclear and cytoplasmic mRNA pools. If decay occurred in the cytoplasm, one would have expected a decrease in the cytoplasmic mRNA pool only. This result could not be explained by any observed differences in rates of transcription or processing of nuclear pre-mRNA or in the rate of cytoplasmic mRNA decay. The results could, however, be explained if the decay pathway is nuclear-associated. For example, nonsense mutations that are utilized during translation in the cytoplasm could trigger decay during transport of the mRNA from the nucleus to the cytoplasm (Belgrader *et al.*, 1993, 1994). This implies that nuclear export and translation may be spacially and temporally coupled, a possibility that remains to be verified experimentally.

One way to see where nonsense mRNA degradation takes place is to determine where gene products that catalyze steps in the pathway localize. At present there is no definitive proof that any of the UPF gene products directly catalyze steps in the pathway. However, we regard UPF1 as a good candidate for direct participation, based on the phenotypes of both dominant and recessive alleles of *UPF1*, and on the presence of structural motifs in the amino acid sequence that suggest a potential for interaction with RNA. We have addressed the question of where UPF1 localizes by developing an immunological detection system for UPF1 based on epitope tagging. Our evidence suggests that yeast UPF1 is present in low abundance throughout the cytoplasm, but is below the limits of cytochemical detection in the nucleus and the mitochondrion. UPF1 has sedimentation properties in sucrose gradients suggesting an association with polyribosomes. The possible functional relationships between the association of UPF1 with polyribosomes and the possible roles of UPF1 and polyribosomes in nonsense mRNA decay are discussed.

MATERIALS AND METHODS

Strains and Genetic Methods

The *S. cerevisiae* strains used in this study are described in Table 1. Strains were constructed using standard yeast genetic techniques (Rose *et al.*, 1990). Media for growth and maintenance of yeast was described by Gaber and Culbertson (1982). Yeast transformations were performed using the method of Ito *et al.* (1983) as described by Ausubel *et al.* (1993). *Escherichia coli* strain DH5α was used for preparation of plasmid DNAs. Methods for growth, maintenance, and transformation of bacteria are described by Sambrook *et al.* (1989).

Nucleic Acid Methods

Plasmid DNA was prepared from *E. coli* by the method of Birnboim and Doly (1979) as described by Sambrook *et al.* (1989). DNA sequence analysis was performed by the method of Sanger *et al.* (1977) using the Sequenase 2.0 kit (United States Biochemical, Cleveland, OH). RNA prepared for Northern analysis was isolated by hot phenol extraction as described by Leeds *et al.* (1991). RNA/DNA hybridizations were carried out by Northern blotting. Total RNA was resolved on 1.0% agarose/formaldehyde gels and blotted onto GeneScreen Plus membranes using the capillary blot protocol recommended by the manufacturer (DuPont, NEN Products, Boston, MA). Hybridization conditions were as described by Klessig and Berry (1983), except that 1.0% sarkosyl was used in the prehybridization and hybridization buffers. DNA probes were prepared from restriction fragments resolved on low-melting point agarose gels and oligolabelled by the method of Feinberg and Vogelstein (1983) using an oligolabelling kit (Pharmacia Biotech, Piscataway, NJ) and [α^{32}P]dCTP (3000Ci/mmol; Amersham, Arlington Heights, IL).

Construction of UPF1–3EP

The influenza virus hemagglutinin (HA) epitope was placed at the C-terminus of UPF1 by in vitro construction of an allele designated *UPF1–3EP*. A 114-bp *Not*I fragment coding for three copies of the nine-amino acid long HA epitope was isolated after *Not*I digestion of plasmid GTEPI (Roof *et al.*, 1992). The *Not*I fragment was placed at the 3′ end of *UPF1* by first creating a *Not*I site between the last sense codon and the termination codon. To accomplish this, a 1473-bp *Ssp*I fragment with end points inside the *UPF1* coding region was deleted from a pUC19 sub-clone that carried the full length *UPF1* gene (designated pUC19UPF1Δ*Ssp*I). Primers 5′-CCC GCG GCC GCC TAT TCC CAA ATT GCT GAA GTC-3′ and 5′-CCC GCG GCC GCT AAT TCG GTG AAC CCT GTT AA-3′ were used in polymerase chain reaction (Ausubel *et al.*, 1993) to create the *Not*I site between the last sense codon and the stop codon of *UPF1*Δ*Ssp*I. Polymerase chain reaction products were analyzed by DNA sequence analysis. The *Not*I fragment coding for the HA epitope was subcloned into the newly introduced *Not*I site of *UPF1*Δ*Ssp*I by standard subcloning procedures. A *Nru*I–*Bam*HI fragment of *UPF1* DNA containing the *Not*I insert was used to replace the wild-type *Nru*I–*Bam*HI fragment in the *UPF1* gene carried on plasmid pRS316, resulting in plasmid pRS316UPF1–3EP. Subsequently, an *Eco*RI–*Bam*HI fragment from pRS316UPF1–3EP containing *UPF1–3EP* was subcloned into pRS314 and pRS315, resulting in plasmids pRS314UPF1–3EP and pRS315UPF1–3EP. pRS314, pRS315, and pRS316 are centromeric plasmids carrying the yeast *TRP1*, *LEU2*, and *URA3* selectable markers, respectively (Sikorski and Hieter, 1989).

Protein Methods

Total protein extracts from yeast were prepared as follows: cultures were grown in 40 ml of -Ura medium at 30°C to a final OD_{600} of 0.6. Cells were pelleted at 8000 × *g* for 10 min and then washed in 10 ml of lysis buffer (5 mM EDTA, 250 mM NaCl, 0.1% Nonidet P-40, 50 mM Tris·HCl, pH 7.4, 4°C). The cell pellet was resuspended in 0.8 ml of lysis buffer plus protease inhibitors (0.1 mM phenylmethylsulfonyl fluoride (PMSF), 1 μg/ml aprotinin, 1 μg/ml pepstatin A, 1 μg/ml chymotrypsin, 1 μg/ml leupeptin, and 1 μg/ml antipain). The cell slurry was divided between two 1.5-ml Eppendorf centrifuge tubes, and lysed with ice cold, acid-washed glass beads by continuous vortexing for 3 min at 4°C. The supernatant was recovered and then cleared by centrifugation for 20 min at 4°C. The amount of protein in the cell lysates was quantitated using a BCA protein quantitation kit (Pierce, Rockford, IL). Twenty micrograms of protein was used for sodium dodecyl sulfate-polyacrylamide gel electrophoresis (SDS-PAGE).

For Western blotting, SDS-PAGE and electrophoretic transfer to nitrocellulose were done using a Bio-Rad Mini-Protean apparatus (Bio-Rad, Hercules, CA) as described by Bollag and Edelstein (1991). Western blotting was done using the ECL Western blotting detection system (Amersham) or as described by Bollag and Edelstein (1991) with modifications. Nitrocellulose blots were decorated with 12CA5 (Berkeley Antibody Company, Richmond, CA), anti-L1 (provided by J. Woolford), anti-RNA1 (provided by A. Hopper), and anti-Hsp60 and anti-hexokinase (provided by G. Schatz) primary antibodies. Secondary antibodies were either a goat anti-mouse IgG antibody-alkaline phosphatase (calf intestine) conjugate or a goat anti-rabbit IgG antibody-alkaline phosphatase (calf intestine) conjugate (Boeringer Mannheim Biochemicals, Indianapolis, IN). Western blots were washed twice in TBST (50 mM Tris·HCl, pH 7.5, 200 mM NaCl, and 0.05% Tween 20), twice in BBST (0.1 M boric acid, 25 mM sodium borate, 1 M sodium chloride, and 0.1% Tween 20) and twice in TBST after incubation with the primary antibody. After incubation with the secondary antibody, blots were washed as previously described except that the final two washes were in TBS (50 mM Tris·HCl, pH 7.5, 200 mM NaCl).

Competition experiments were performed as described above, except that HA competitor peptide (YPYDVPDYA; Multiple Peptide Systems, San Diego, CA) containing the epitope recognized by the 12CA5 antibodies was added to the primary antibody-binding buffer.

Indirect Immunofluorescent Microscopy

Ten milliliter cultures of yeast were grown to mid-log phase (OD_{600} = 0.4–0.7) in medium to select for the presence of plasmids carrying the *UPF1–3EP* gene. Next, 1.4 ml of 37% formaldehyde was added and the culture was incubated at 37°C for 5 min with gentle shaking. The culture was then allowed to sit at room temperature for 1 h. The cells were pelleted for 2 min at 300 × *g* and then washed three times in 3 ml of buffer 1 (1.2 M sorbitol, 0.1 M potassium phosphate, pH 6.5, 1% β-mercaptoethanol). Cells were resuspended in 0.5 ml of buffer 1 and 50 U of lyticase was added followed by incubation for 9 min at 30°C with gentle shaking. The cells were pelleted and washed twice with 3 ml of buffer 2 (1.2 M sorbitol, 0.1 M potassium phosphate, pH 6.5). Cells were resuspended in buffer 2 to approximately A_{600} = 5.0/ml. Cells (60 μl) were spotted onto slides pretreated with 1% polyethyleneimine. The cells were allowed to settle for 30 min and then the slides were rinsed twice in phosphate-buffered saline (PBS). The slides were then immersed in methanol (pre-chilled to −20°C) for 6 min followed by immersion in acetone (chilled to −20°C) for 30 s. Slides were air dried. Cells were blocked with 30 μl of blocking buffer (1% bovine serum albumin and 0.05% Nonidet P-40 in PBS) for 15 min at room temperature. Thirty microliters of PBS containing the primary antibodies was added and the slides were incubated overnight at room temperature. Slides were washed twice in 0.5% Nonidet P-40, PBS and then three times in PBS. The cells were blocked again as described above, followed by the addition of 30 μl of PBS containing the secondary antibodies. The slides were incubated for 1 h at room temperature and then washed as previously described. The DNA was stained with 4,6-diamidino-2-phenylindole (DAPI) by adding 30 μl of 1 μg/ml DAPI, incubating the slides for 5 min at room temperature, and then rinsing twice in PBS. The slides were allowed to air dry. Once dry, the cells were mounted in 0.1% phenylenediamine. Slides were viewed using a Fluor 100X oil immersion lens on a Nikon optiphot biological microscope adapted for fluorescence microscopy with a microflex UFX-IIA photomicrographic attachment (Nikon, Garden City, NY), and a Zeiss/IM35 (Thornwood, NY) equipped with a Bio-Rad MRC600 Lasersharp Confocal system.

UPF1–3EP was detected with the 12CA5 antibodies obtained from the Berkeley Antibody Company. SEN1::βgal was detected by polyclonal antibodies against the βgal portion of the fusion and were obtained from S. Blair. KAR2, L1, and MAS2 antibodies were obtained from M. Rose, J. Woolford, and E. Craig, respectively. Secondary antibodies were either a goat anti-mouse IgG fluorescein conjugate or a goat anti-rabbit IgG-L-rhodamine conjugate (Boehringer Mannheim Biochemicals).

Cell Fractionation

Cells were fractionated and a crude ribosome pellet was prepared using the method of Grant *et al.* (1974) with modifications from Sachs and Davis (1989). Part of the cell lysate (150 μl) was reserved as a total cellular extract. The remaining 1 ml cell lysate was centrifuged at 5,000 × *g* for 5 min. The supernatant (cytosol-enriched fraction) was transferred to a fresh tube and the pellet was resuspended in 1 ml of Laemmli buffer supplemented with 4.5 M urea. The ribosomes were pelleted from 600 μl aliquots of the cytosol-enriched fraction by centrifugation at 160,000 × *g* for 90 min. The supernatant was transferred to a fresh Eppendorf tube, and the pellet was resuspended in 600 μl of Laemmli buffer supplemented with 4.5 M urea.

Cells were fractionated into mitochondrial and post-mitochondrial fractions essentially as described by Herbert *et al.* (1988), except that crude mitochondria were washed four times in the presence of 1 mM PMSF followed by two washes in the absence of PMSF.

Mitochondria were treated with 0.2 mg/ml proteinase K for 30 min on ice. Where indicated, mitochondria were solubilized by addition of Triton X-100 to 0.5%. Proteinase K digestion was terminated by adding PMSF to 1 mM.

Polyribosome Analysis

Polyribosomes were prepared and fractionated as described by Deshmukh *et al.* (1993) with the following modifications. Washed cells were suspended in 0.8 μl of lysis buffer. Where indicated the cycloheximide was omitted from the lysis buffer. For RNase disruption of polyribosomes, 5 μl of a 10 mg/ml RNase A was added to 200 μl polyribosomes isolated in the absence of DEPC with or without the addition of 50 μg/ml cycloheximide and incubated for 15 min on ice before loading onto sucrose gradients. Growth conditions were altered by shifting cells grown in −Trp medium into YEPD at an OD_{600} of 0.1. Cell were harvested at an OD_{600} of 0.4. Plasmid loss was monitored by plating onto YEPD at the time cells were harvested and then replica plating onto -Trp plates. Aliquots of 20–25 A_{260} units of cell lysate were loaded onto 12 ml, 7–47% sucrose gradients and subjected to centrifugation at 39,000 rpm for 2.5 h in a SW41 rotor (Beckman Instruments, Fullerton, CA). The OD_{254} profile of the gradient was determined with an ISCO UA-6 detector (Lincoln, NE) equipped with a density gradient flow cell. Fractions (0.5 ml) were collected using an ISCO Foxy Jr. fraction collector. The proteins in the fractions were acetone precipitated, and then resuspended in 10 μl of Laemmli buffer supplemented with 4.5 M urea. Samples were fractionated by SDS-PAGE and transferred to membranes for Western blotting using the ECL Western blotting detection system (Amersham). The bands on autoradiographs of the Western blots were quantitated using a Model 300A computing densitometer (Molecular Dynamics, Sunnyvale, CA). Hyperfilm ECL (Amersham) was pre-flashed before autoradiography and only bands within the linear dynamic range were quantitated. The density of the bands on autoradiographs and the concentration of protein in the bands is not directly proportional because the emission of light from ECL Western blots is nonlinear. As a consequence of this, the peak accumulation of protein is underestimated using this technique.

RESULTS

The aim of this study was to determine the intracellular localization of UPF1. Using immunological detection, we determined localization by three methods: indirect immunofluorescence, cell fractionation, and distribution relative to polyribosomes fractionated in a sucrose gradient. To detect UPF1 in these experiments, the wild-type gene was modified by placing a DNA sequence immediately 5′ to the normal termination codon that codes for three tandem copies of the 12CA5 influenza virus HA epitope (see MATERIALS AND METHODS). The modified gene, designated *UPF1–3EP*, was subcloned into centromeric plasmids and introduced into strains PLY38, BJ2168, and PLY102 (Table 1). PLY38 and PLY102 both lack a functional *UPF1* gene. BJ2168 carries a wild-type *UPF1* gene. The experiments described below were performed using these strains.

A C-Terminal Epitope-tagged UPF1 Product Is Functional In Vivo

The ability of *UPF1–3EP* to provide wild-type UPF1 function in vivo was tested using a frameshift allosuppression assay described previously in which the rate of growth on medium lacking histidine is sensitive to the turnover rate of *his4–38* mRNA (Culbertson *et al.*, 1980; Leeds *et al.*, 1991). Strains wild type for the *UPF* (up frameshift) genes and carrying both *his4–38* and *SUF1–1* have a His^+ phenotype at 30°C, but these cells remain His^- at 37°C. Mutations in *UPF1* confer a His^+ phenotype at 37°C through restabilization of *his4–38* mRNA. Using this assay (Figure 1A), we found that the growth of strain PLY38[pRS316UPF1–3EP] at 37°C was somewhat faster but very similar to strain PLY38[pRS316UPF1]. However, strain PLY38-[pRS316], which lacks both *UPF1* and *UPF1–3EP*, grew rapidly to confluency at 37°C. These growth tests indicate that *UPF1–3EP* confers nearly complete complementation of the loss of wild-type UPF1 function.

The function of UPF1–3EP was compared with UPF1 using quantitative Northern blotting to determine the effect of each gene on *his4–38* mRNA accumulation. The relative levels of *his4–38* mRNA accumulation in strain PLY38 transformed separately with pRS316, pRS316UPF1, and pRS316UPF1–3EP were 1.0, 0.47 (± 0.03), and 0.55 (± 0.06), respectively. Thus, UPF1–3EP reduced *his4–38* mRNA accumulation 86% (± 5%) as well as the wild-type UPF1 protein. Because

Table 1. Yeast strains

Strain	Genotype	Source
PLY22	*MAT***a** *ura3-52 his4-38 SUF1-1 met14*	This study
PLY38	*MAT***a** *upf1-2*[a] *his4-38 SUF1-1 ura3-52*	This study
PLY102	*MAT***a** *upf1-Δ1 ura3-52 trp1-7 leu2-3,-112*	Leeds *et al.*, 1991
PLY142	*MAT***a** *his4-38 SUF1-1 upf1-Δ1 ura3-52 trp1-Δ1 leu2-1*	This study
BJ2168	*MAT***a** *ura3-52 leu2 trp1 prc1-407 prb1-1122 pep4-3 gal2*	E. Jones
CW04	*MATα his3-11 leu2-3,112 ade2-1 ura3-1 trp1-1 can1-100 UPF1 (rho+, mit+)*	Altamura *et al.*, 1994
CNA	*MATα his3-11 leu2-3,112 ade2-1 ura3-1 trp1-1 can1-100 upf1-Δ3 (rho+, mit+)*	Altamura *et al.*, 1994

[a]The mutation in *upf1-2* is a single nucleotide change at nucleotide +615 that changes a UGG Trp codon to a UGA nonsense codon. This allele of *UPF1* has a phenotype that is indistinguishable from a null allele of *UPF1* (Leeds *et al.*, 1992).

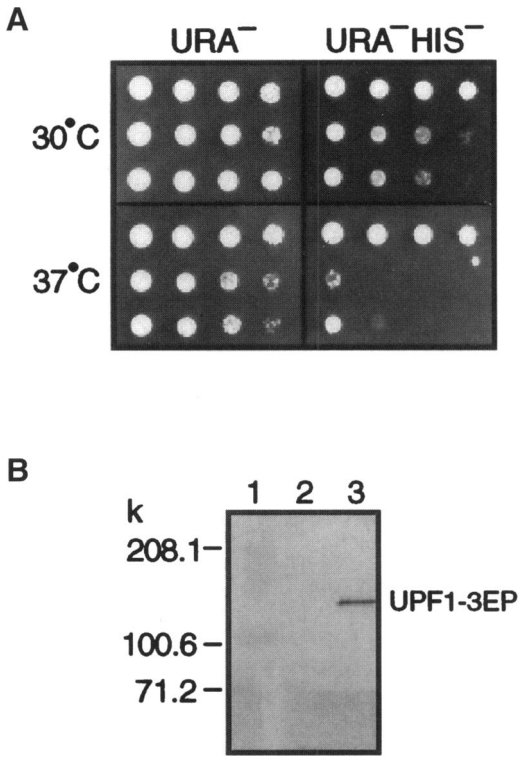

Figure 1. (A) In vivo complementation. Growth tests were performed to assess the ability of UPF1–3EP to compensate for loss of wild-type UPF1 function. Strains carrying the suppressible frameshift mutation *his4–38* (Donahue *et al.*, 1981), the tRNA frameshift suppressor *SUF1–1* (Mendenhall *et al.*, 1987), and a wild-type *UPF1* gene fail to grow at 37°C on −histidine medium due to destabilization of *his4–38* mRNA (Leeds *et al.*, 1991). Equivalent strains carrying a *UPF1* loss-of-function mutation grow at 37°C on −histidine medium due to re-stabilization of *his4–38* mRNA (Culbertson *et al.*, 1980; Leeds *et al.*, 1991). Strain PLY38, which carries the *upf1–2* allele (Table 1), was separately transformed with three centromeric plasmids carrying the yeast *URA3* gene: pRS316 (no *UPF1* gene), pRS316UPF1 (wild-type *UPF1* gene), and pRS316UPF1–3EP (epitope-tagged *UPF1* gene). Growth of the resulting transformants was tested by plating 10^0, 10^{-1}, 10^{-2}, and 10^{-3} serial dilutions of overnight cultures on −Ura and −Ura −His medium at 30°C and 37°C. Rows 1 and 4 show the extent of growth of PLY38[pRS316]. Rows 2 and 5 show the extent of growth of PLY38[pRS316UPF1]. Rows 3 and 6 show the extent of growth of PLY38[pRS316UPF1–3EP]. Identical results were obtained using transformants of strain PLY142 carrying *upf1-Δ1*. (B) Immuno-detection of UPF1–3EP on Western blots using 12CA5 antibodies. The blots were prepared using total protein extracts from strain BJ2168 (Table 1) transformed with plasmid pRS316 (lane 2) and pRS316UPF1–3EP (lane 3). Pre-stained molecular weight markers were loaded in lane 1.

his4–38 mRNA accumulation is proportional to half-life in PLY38 transformants (Leeds *et al.*, 1991), the levels of accumulation reflect how well UPF1–3EP promotes nonsense mRNA decay. Furthermore, the UPF1–3EP phenotype is recessive to wild type, indicating that the modestly reduced function of UPF1–3EP could result from a reduction in the amount of UPF1 protein or a partial loss of function. Based on these results, the behavior of UPF1–3EP is expected to resemble that of the wild-type UPF1 protein and is therefore suitable for localization studies.

The product of the *UPF1–3EP* gene was detected as a single band with an approximate molecular weight of 113 k on a Western blot of protein from strain BJ2168[pRS316UPF1–3EP] probed with 12CA5 antibodies (Figure 1B). The estimated molecular weight of this band based on its migration in SDS-polyacrylamide gels relative to molecular weight standards agrees well with the molecular weight for UPF1–3EP predicted from the DNA sequence. This band was not detected in protein derived from strain BJ2168-[pRS316], which lacks the *UPF1–3EP* gene. These results suggest that the observed band is the product of the *UPF1–3EP* gene. No other bands are detectable using the Western blotting conditions described in MATERIALS AND METHODS. To further substantiate these conclusions, a peptide competition experiment was performed. Increasing concentrations of free peptide containing the 12CA5 epitope diminished the 113-k signal on Western blots. Therefore, the observed band results from the recognition of UPF1–3EP by 12CA5 antibodies (our unpublished observations).

As a final test of the experimental system, we performed indirect immunofluorescent microscopy using 12CA5 antibodies. Strain PLY102[pRS314UPF1–3EP] gave a visible fluorescent signal, whereas PLY102-[pRS316] did not (our unpublished observations). This result indicates that background fluorescence was sufficiently low to allow cells expressing UPF1–3EP to be used to localize the protein.

UPF1–3EP Is Cytoplasmic

UPF1–3EP was localized by indirect immunofluorescence in cells double-labeled with antibodies against UPF1–3EP and L1, a SEN1::βgal fusion, KAR2, or MAS2. L1, a component of the 60S ribosomal subunit (Deshmukh *et al.*, 1993), is located primarily in the cytoplasmic ribosomes. A small amount of L1 is also found in the nucleolus where ribosomal subunits are assembled. SEN1::βgal localizes to the nucleus (Ursic, DeMarini, and Culbertson, unpublished data; DeMarini *et al.*, 1992). KAR2 localizes to the endoplasmic reticulum (ER) (Rose *et al.*, 1989). Because the ER is contiguous with the nuclear membrane in yeast, fluorescence due to KAR2 often forms a ring that marks the boundary between the cytoplasm and the nucleus (Rose *et al.*, 1989). Eighty percent of the cells stained with KAR2 antibodies had a ring marking the boundary between the cytoplasm and the nucleus (our unpublished observations). MAS2 is found in the mitochondrial matrix (Jensen and Yaffe, 1988).

Figure 2 shows a comparison of representative cells stained with antibodies against L1, SEN1::βgal, KAR2, MAS2, and UPF1–3EP. DNA was visualized by staining with DAPI. The staining pattern with 12CA5 antibodies that recognize UPF1–3EP is characteristic of a protein localized to the cytoplasm. The region with the least intense 12CA5 staining corresponds to the region of intense DAPI staining. DAPI marks the location of chromosomal DNA. Staining with anti-βgal and anti-KAR2 antibodies shows the location of the nucleoplasm and the nuclear/cytoplasmic boundary, respectively. These results indicate that UPF1–3EP is primarily localized in the cytoplasm. From these experiments, UPF1–3EP does not co-localize exclusively with the mitochondrial protein MAS2. The possibility that some UPF1–3EP might localize to the mitochondrion was addressed in subsequent experiments using confocal microscopy and fractionation.

Confocal microscopy was used to further resolve any potential overlap in the distribution of UPF1–3EP with L1, SEN1::βgal, KAR2, and MAS2 (Figure 3). 12CA5 antibodies were used to visualize UPF1–3EP using fluorescein-conjugated secondary antibodies (Figure 3, left column). These cells appear to stain mostly green, but with some regions where no staining is visible. To determine if the unstained regions correspond to the nuclei, we examined overlays of images showing UPF1–3EP staining with images of rhodamine-stained SEN1::βgal or KAR2 (red) (Figure 3, B and C). Any overlap in staining pattern appears as yellow. Very little overlap in the staining pattern of UPF1–3EP and SEN1::βgal or KAR2 was observed, indicating that there is little or no detectable UPF1–3EP in the nucleus. Also, there was very little overlap in the staining pattern of UPF1–3EP and MAS2, the mitochondrial matrix protein (Figure 3D). In contrast, an intense yellow color indicates significant overlap in distribution between UPF1–3EP and ribosomal protein L1 (Figure 3A). We cannot rule out the possibility that there may be small amounts of UPF1–3EP in the nucleus, ER, or mitochondria, but if

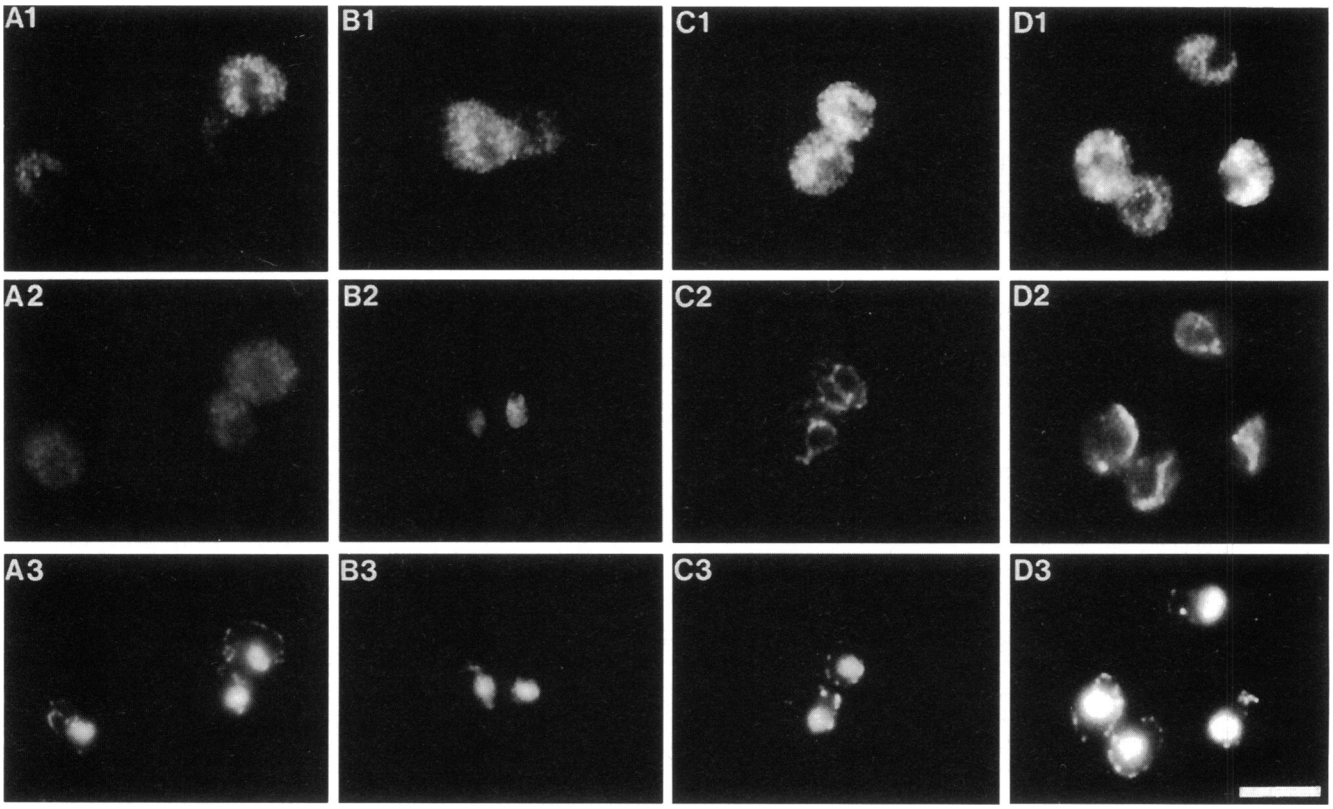

Figure 2. UPF1–3EP is localized in the cytoplasm. Strain PLY102 (Table 1) was transformed with centromeric plasmid pRS314UPF1–3EP. Cells were stained with DAPI (bottom row: A3, B3, C3, and D3) and with 12CA5 antibodies that recognize UPF1–3EP (top row: A1, B1, C1, and D1). The middle row shows cells stained with antibodies that recognize L1 (A2), SEN1::βgal (B2), KAR2 (C2), and MAS2 (D2). L1 is primarily localized in the cytoplasm, SEN1::βgal in the nucleus, KAR2 in the endoplasmic reticulum, and MAS2 in the mitochondrion (Jensen and Yaffe, 1988; Rose *et al.*, 1989; Deshmukh *et al.*, 1993; Ursic, DeMarini, and Culbertson, unpublished data). The SEN1::βgal fusion, which is expressed from a GAL1 promoter on a 2 μ plasmid, was induced by pre-growth in raffinose followed by growth in galactose-containing medium. Bar, 5 mm.

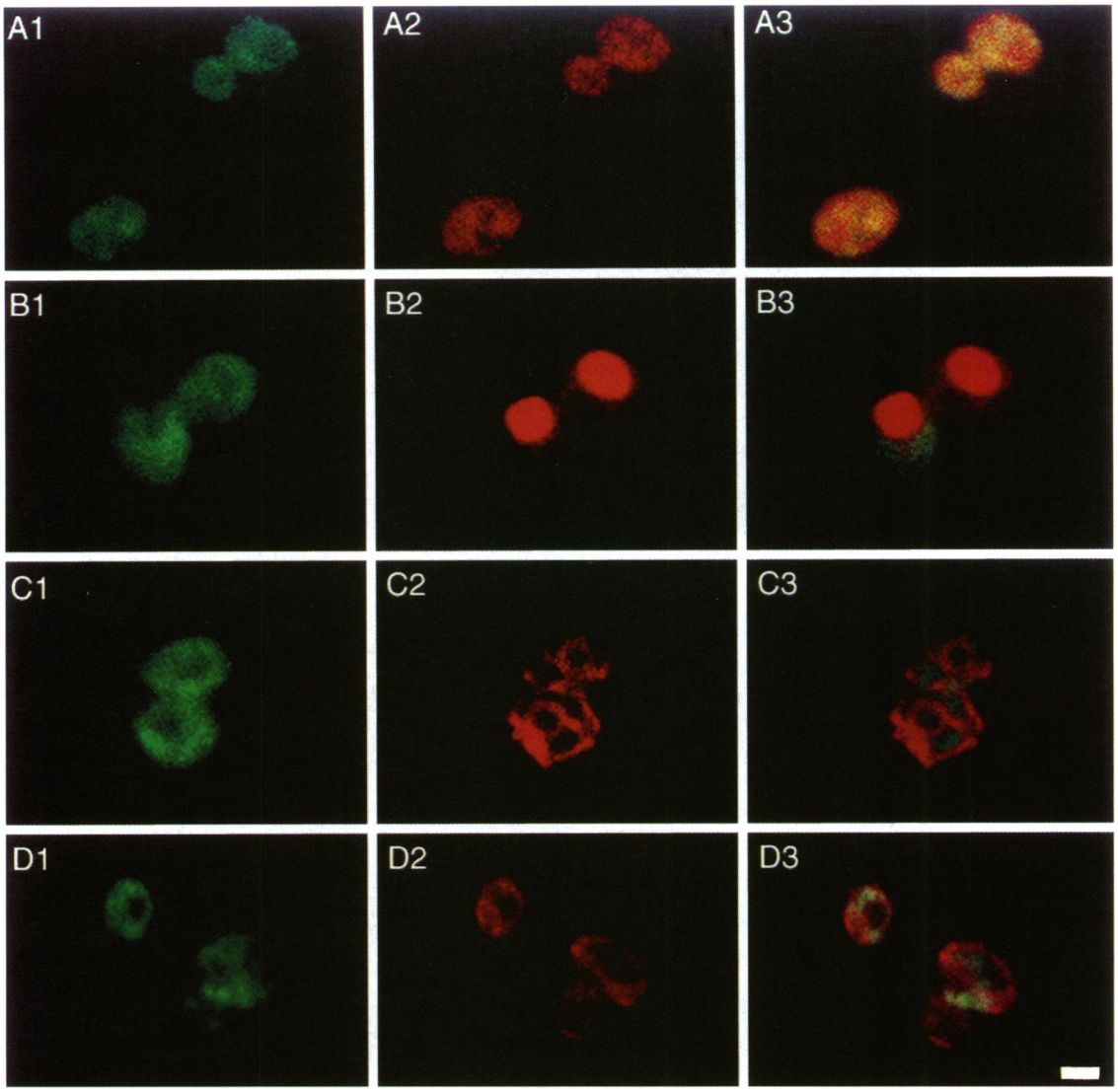

Figure 3. The distribution of UPF1–3EP overlaps with ribosomal protein L1. Strain PLY102 (Table 1), was transformed with the centromeric plasmid pRS314UPF1–3EP. Cells were stained with 12CA5 antibodies that recognize UPF1–3EP using fluorescein-conjugated secondary antibodies (first column, green) and with antibodies that recognize L1 (A2), β-gal (B2), KAR2 (C2), or MAS2 (D2) using rhodamine-conjugated secondary antibodies (second column, red). Staining was visualized by confocal microscopy. Single images from the first and second columns were overlaid to determine the extent of co-distribution [UPF1–3EP and L1 (A3), SEN1::βgal (B3), KAR2 (C3), and MAS2 (D3)]. The regions of co-localization appear as yellow. Bar, 2 mm.

present in these compartments it must be at concentrations below the level of detection using this approach.

UPF1–3EP Fails to Accumulate in Mitochondria

The *UPF1* gene isolated by Leeds *et al.* (1992) on the basis of allo-frameshift suppression (Leeds *et al.*, 1991) was also identified as *NAM7* by Altamura *et al.* (1992) in a screen for multi-copy suppressors of a mitochondrial splicing-deficient mutation (Ben Asher *et al.*, 1989). Although *UPF1* is not essential for growth in glucose-containing medium (Leeds *et al.*, 1992), loss of UPF1 function causes respiratory impairment and slow growth in lactate-containing medium (Altamura *et al.*, 1992) (Figure 4A). These results suggest a potential function for UPF1 in the mitochondrion. To investigate this observation further, cell lysates were fractionated using a method that separates the mitochondria from the cytoplasm (see MATERIALS AND METHODS). The fractions were examined by Western blotting using antibodies that recognize UPF1–3EP, the mitochondrial matrix protein Hsp60,

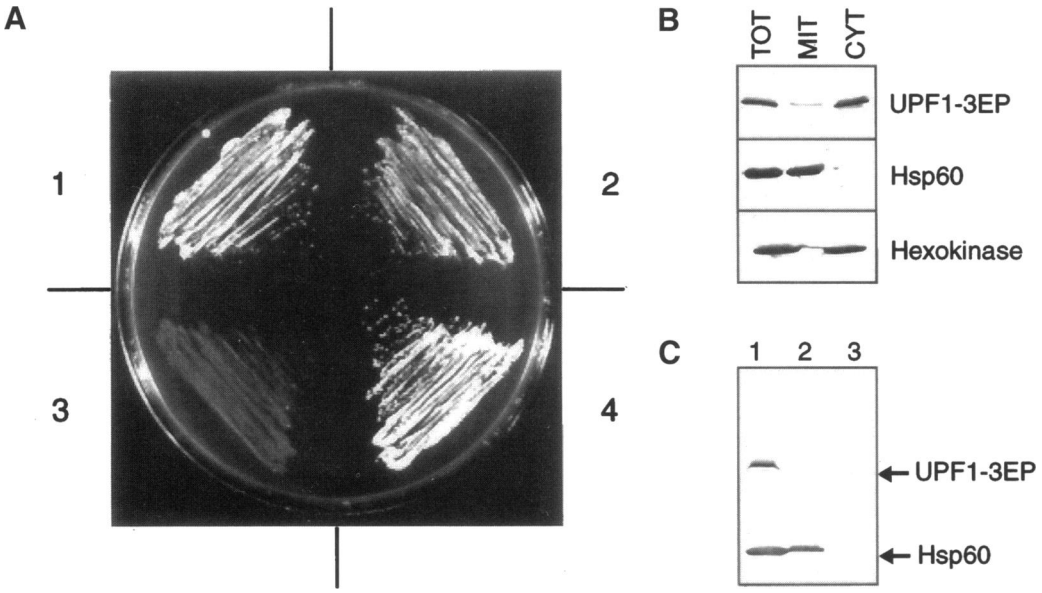

Figure 4. *UPF1–3EP* complements respiratory deficiency, but the UPF1–3EP protein fails to accumulate in mitochondria. Strains carrying a *upf1::URA3* null allele fail to grow on medium containing lactate as the sole carbon source at 18°C (Altamura *et al.*, 1992). We tested whether *UPF1–3EP* can suppress the growth defect caused by a *upf1::URA3* null allele in strain CNA (Table 1), and whether any UPF1–3EP can be detected in the mitochondrion. (A) Transformants of strain CNA (Table 1) carrying different *UPF1* alleles on centromeric plamids were grown on medium containing lactate as the sole carbon source for 12 days at 18°C, as follows: (1) CNA [pRS315UPF1], (2) CNA [pRS315UPF1–3EP], (3) CNA [pRS315], which does not carry any UPF1 sequences, and (4) CW04, an isogenic wild-type strain carrying the *UPF1* gene. The results indicate that *UPF1–3EP* suppresses the growth defect conferred by the *upf1::URA3* null allele, and it supports growth on lactate medium in a manner similar to *UPF1*. (B and C) Mitochondrial and cytoplasmic fractions were prepared from strain PLY102 (Table 1) transformed with pRS314UPF1–3EP (see MATERIALS AND METHODS). Fractions were analyzed by SDS-PAGE and Western blotting using antibodies that recognize UPF1–3EP, the mitochondrial matrix protein Hsp60, and the cytoplasmic protein hexokinase. Lanes in panel B were loaded as follows: TOT, 150 μg of total extract; MIT, 30 μg of the mitochondrial fraction; CYT, 113 μg of the post-mitochondrial fraction. Lanes in panel C were loaded with 100 μg of the mitochondrial fraction treated as follows: Lane 1, untreated; lane 2, addition of 0.2 mg/ml proteinase K; lane 3, solubilization in 0.5% Triton X-100 followed by the addition of 0.2 mg/ml proteinase K.

and the cytoplasmic protein Hexokinase (Figure 4B). Most of the detectable Hsp60 and a small amount of Hexokinase were found in the mitochondrial fraction, whereas no Hsp60 and the majority of Hexokinase were found in the cytoplasmic fraction. The fractionation of UPF1–3EP resembled that of Hexokinase.

Mitochondria were treated with proteinase K to determine whether the small amount of UPF1–3EP in the mitochondrial fraction is located inside or outside of the mitochondrion. After proteinase K treatment of the mitochondrial fraction, UPF1–3EP was no longer detectable, whereas Hsp60 was readily detected (Figure 4C). This shows that UPF1–3EP is outside the mitochondrion. The lack of growth on lactate-containing medium, which is indicative of respiratory impairment, probably is an indirect consequence of UPF1 function outside the mitochondrion.

UPF1–3EP Is Associated with Polyribosomes

Cell fractionation experiments indicated that a significant portion of the detectable UPF1–3EP co-fractionates with L1, and hence, with ribosomes (our unpublished observations). To determine whether UPF1–3EP is specifically associated with ribosomes, its distribution was compared with the distribution of L1 in polyribosomes fractionated in a 7–47% sucrose gradient (see MATERIALS AND METHODS and Figure 5). Protein extracts were prepared from cells grown in −Trp synthetic medium to select for the presence of the plasmid carrying *UPF1–3EP*. To arrest translational elongation, 50 μg/ml cycloheximide was added to the growth medium immediately before harvesting the cells. Cycloheximide was also included at the same concentration in the lysis buffer to prevent ribosome runoff during extract preparation. The extracts were resolved into 40S and 60S ribosomal subunits, 80S ribosomal particles, and polyribosomes (Figure 5A). Western blots prepared from fractions recovered from the sucrose gradients were sequentially labeled with antibodies to detect UPF1–3EP and L1. Autoradiographs of the blots were quantitated using the ECL Western blotting detection system (Amersham). Light emission by ECL is nonlinear, consequently the peak

accumulation of proteins by this technique is underestimated (see MATERIALS AND METHODS). Using these conditions, approximately 80% of UPF1–3EP was detected in fractions 8–24+P (P = pellet). These fractions contain ribosomal subunits, 80S particles and polyribosomes. About 20% was detected in fractions 1–7 from the top of the gradient where monomeric proteins, smaller aggregates, and complexes are expected to migrate. Virtually all of the detectable L1, a component of the 60S ribosomal subunit, was found in fractions 8–24+P. These fractions include the 60S ribosomal subunits, the 80S particles and the polyribosomes. In the fractions 8–24+P that contain the 80S ribosomal particle and the polyribosomes, UPF1–3EP and L1 have a very similar distribution. These results indicate that a significant proportion of UPF1–3EP is part of a high molecular weight aggregate or complex that co-distributes with polyribosomes.

Strains carrying a *upf1*$^-$ null mutation are hypersensitive to cycloheximide (Leeds *et al.*, 1992). To test the possibility that the addition of cycloheximide to the growth medium and the lysis buffer affects the sedimentation profile of UPF1–3EP, extracts were prepared using a range of cycloheximide concentrations. Using 25–50 μg/ml cycloheximide, the A_{254} profile and the distribution of UPF1–3EP across the sucrose gradient resembled the profile and distribution shown in Figure 5A. In the presence of 100–200 μg/ml cycloheximide, the A_{254} profiles were unaltered but the amount of UPF1–3EP distributed across the gradient appeared to be reduced (our unpublished observations). These results indicate that 50 μg/ml cycloheximide can be used in the preparation of polyribosomes without significantly affecting the distribution of UPF1–3EP.

Conditions known to affect the distribution of polyribosomes on sucrose gradients also affected the distribution of UPF1–3EP and L1. In Figure 5B, cycloheximide was omitted during polyribosome preparation. The omission of cycloheximide allows translation on the polyribosomes to be completed (Ramirez *et al.*, 1991). Because new rounds of initiation are infrequent during cell harvest and extract preparation, 80S ribosomes and the 40S and 60S subunits accumulate at the expense of polyribosomes (Ramirez *et al.*, 1991). The majority of the ribosomal subunits were present in 80S particles as judged by the A_{254} profile, but detectable amounts of polyribosomes remained intact, as judged from the A_{254} profile and the fact that 45% of L1 was still found in the fractions containing the polyribosomes (14–24+P). Similar amounts of UPF1–3EP also extend into the polyribosome region of the gradient. The amounts of UPF1–3EP and L1 in fractions 14–24+P were each reduced by about 20% compared with extracts prepared in the presence of cycloheximide. The remainder of UPF1–3EP and L1 was detected in fractions 8–13, which contain the 40S and 60S ribosomal subunits and the 80S ribosomal particles. In the absence of cycloheximide, very little UPF1–3EP or L1 was observed in fractions near the top of gradient. Thus, UPF1–3EP and L1 have very similar distributions.

Cell extracts isolated in the presence or absence of cycloheximide (Figure 5, C and D) were treated with 0.5 mg/ml RNase A before fractionation to disrupt the polyribosomes. Using these conditions the majority of the ribosomes were present in 80S particles as judged by the A_{254} profile. Western blots show that the majority of L1 accumulates at a position coincident with the 80S particles. Only 15–20% of L1 migrates in the polyribosome region (fractions 14–24+P). Similarly, only about 10% of UPF1–3EP migrated into this region of the gradient. Two separate regions of peak accumulation were observed for UPF1–3EP. One corresponds to monomers, small aggregates, and complexes (about 55% in fractions 1–7 irrespective of the presence or absence of cycloheximide). The other peak location was coincident with the 40S and 60S ribosomal subunits and the 80S ribosomal particle (about 35% in fractions 8–13 irrespective of the presence or absence of cycloheximide). Overall, RNase A treatment results in a 65–85% reduction in the amount of UPF1–3EP and L1 found in fractions where polyribosomes migrate. A commensurate increase in accumulation of these proteins was observed in fractions containing monomers, smaller molecular weight aggregates and complexes, 40S and 60S ribosomal subunits, and 80S ribosomal particles.

Growth conditions affect the relative ratio of 80S ribosomal particles to polyribosomes. Cells grown in −Trp synthetic medium were shifted to YEPD medium for two cell generations before extraction in the presence of 50 μg/ml cycloheximide (Figure 5E; MATERIALS AND METHODS). Under these nonselective conditions, 75% of the cells retained the plasmid carrying *UPF1–3EP*. Polyribosomes accumulate at the expense of 80S ribosomal particles as judged by the A_{254} profile and the distribution of L1. About 80% of the L1 was detected in the polyribosome fractions (14–24+P), whereas 75% of UPF1–3EP was detected in these fractions. Growth in YEPD results in a 30% and a 20% increase in the amounts of L1 and UPF1–3EP, respectively, in polyribosome fractions compared with growth in -Trp synthetic medium. Approximately 5% of UPF1–3EP was found in fractions 1–7 where monomers and small complexes migrate and 20% in fractions 8–13 where the 40S and 60S ribosomal subunits and 80S ribosomal particles migrate. Compared with Figure 5A, these results demonstrate that UPF1–3EP and L1 exhibit a similar shift in distribution in the polyribosome region when cells are grown in medium that supports rapid growth.

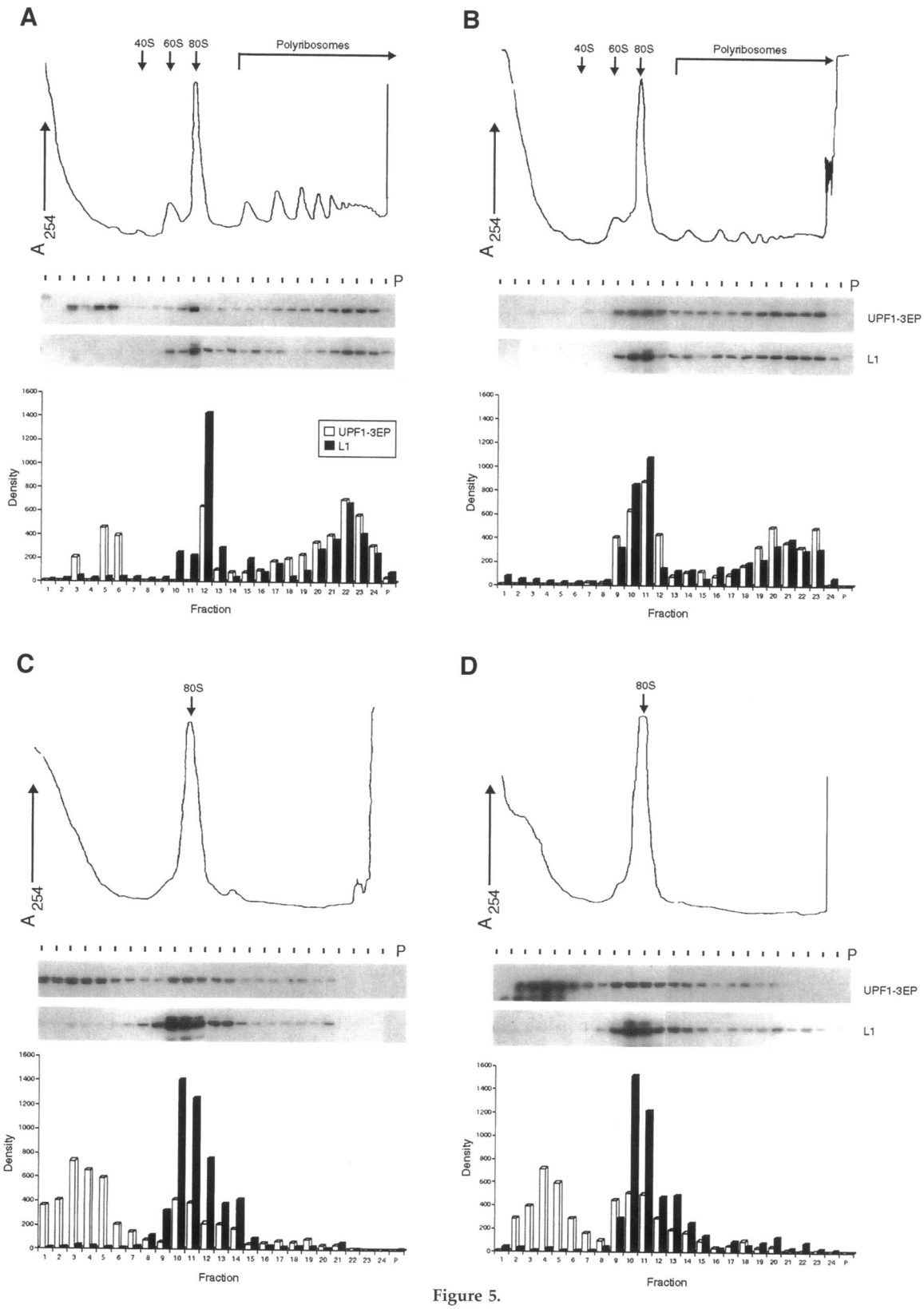
A
40S 60S 80S
Polyribosomes
A 254
P
UPF1-3EP
L1
Density
Fraction
B
40S 60S 80S
Polyribosomes
A 254
P
UPF1-3EP
L1
Density
Fraction
C
80S
A 254
P
Density
Fraction
D
80S
A 254
P
UPF1-3EP
L1
Density
Fraction

Figure 5.

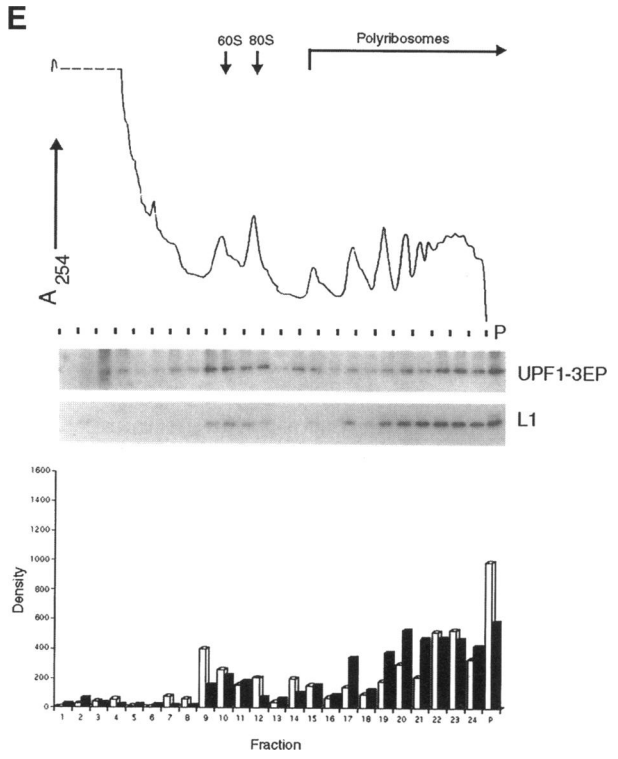

Figure 5 cont. Strain PLY102 (Table 1) was transformed with pRS314UPF1–3EP and grown in -Trp synthetic medium (MATERIALS AND METHODS). Cell extracts were separated on 7–47% sucrose gradients as follows: in the (A) presence of 50 μg/ml cycloheximide, in the (B) absence of cycloheximide, after treatment with RNase A following isolation in the (C) presence of 50 μg/ml cycloheximide or in the (D) absence of cycloheximide, and (E) prepared from cells shifted to YEPD for two cell generations before harvest in the presence of 50 μg/ml cycloheximide. Approximately 75% of the cells shifted to YEPD contained the plasmid at harvest (see MATERIALS AND METHODS). The gradients were monitored by absorbance at A_{254}. Fractions taken from the gradients were resolved on 10% polyacrylamide SDS gels. Western blots prepared from the gels were sequentially labeled with antibodies to detect UPF1–3EP and L1 using the ECL Western blotting detection system (Amersham). The distribution of UPF1–3EP and L1 was determined by quantitation of autoradiographs of Western blots using a computing densitometer (see MATERIALS AND METHODS). The the amounts of UPF1–3EP and L1 in each fraction are shown with white and black bars, respectively. Solubilized pellets from the sucrose gradients (P) were included on the right of each panel. The positions of 40S and 60S ribosomal subunits, 80S ribosomal particles, and polyribosomes are also indicated.

Based on the changes in distribution observed for UPF1–3EP and L1 using three different sets of conditions that alter the polyribosome profile, we suggest that UPF1–3EP associates with polyribosomes.

The Relative Abundance of UPF1

Given the evidence that UPF1–3EP associates with polyribosomes, we wanted to estimate the ribosome/UPF1 molar ratio. Because no tools are yet available to determine the ratio at the protein level, we measured the accumulation of *UPF1* mRNA relative to the accumulation of ribosomal protein S3 and L3 mRNA. S3, a component of the 40S ribosomal subunit, is encoded by the *SUF14* gene (Hendrick and Culbertson, unpublished data). L3, a component of the 60S subunit, is encoded by the *TCM1* gene (Fried and Warner, 1981). In yeast, ribosomal protein gene expression is coordinately controlled to ensure equimolar accumulation (reviewed in Woolford and Warner, 1991). Because coordinate control is predominantly transcriptional, we expect that the accumulation of mRNAs encoding different ribosomal proteins will be roughly equivalent and proportional to the accumulation of 40S and 60S ribosomal subunits and 80S ribosomes. Assuming that the mRNAs are all translated at similar rates, the relative ratios of UPF1, S3, and L3 mRNA should give an indication of UPF1 abundance relative to ribosomes.

To compare levels of mRNA accumulation, total RNA extracted from strain PLY22 (Table 1) during early, middle, and late logarithmic growth was probed by Northern blotting. PLY22 carries the intron-less *UPF1*, *SUF14*, and *TCM1* genes in single copy at their normal chromosomal locations. The length and G+C content of uniformly labeled DNA probes from the coding regions of each gene were as follows: *UPF1*, 2305-bp, 39.5% G+C; *SUF14*, 652-bp, 44.0% G+C; *TCM1*, 1097-bp, 43.8% G+C. The amount of radioactivity detected in the DNA/RNA hybrids, which corresponded to visible bands detected by autoradiography, was adjusted for probe length as described in Table 2. The effects of small differences in G+C content were considered negligible.

The results of Northern blotting indicate that UPF1 mRNA is much less abundant than S3 or L3 mRNA (Table 2). The average accumulation ratios for S3/UPF1 and L3/UPF1 mRNA are approximately 120 and 90, respectively. The S3/L3 mRNA ratio was 1.3, close to a theoretically expected ratio of 1.0. These results indicate that UPF1 mRNA accumulates at a much lower level than two ribosomal protein mRNAs. On this basis, we suggest that the UPF1 protein may be relatively nonabundant compared with ribosomes.

DISCUSSION

UPF1 Is Located Primarily in the Cytoplasm

We anticipated that UPF1 might be located in one or more of several different intracellular compartments, including the cytoplasm, the nucleus, or the mitochondrion.

A cytoplasmic location was suggested by evidence that nonsense mRNAs subject to UPF1-mediated decay are found in polyribosomes, which are primarily

Table 2. Relative abundance of UPF1 mRNA[a]

Growth phase	OD_{600}	mRNA accumulation ratio[b] S3/UPF1	L3/UPF1	S3/L3
Early log	0.27–0.30	118.3 (11.6)	93.8 (7.8)	1.3 (0.04)
Mid-log	0.51–0.54	118.9 (11.7)	88.0 (9.9)	1.3 (0.04)
Late log	1.5–1.6	123.5 (12.7)	87.7 (10.1)	1.4 (0.04)

[a]Total RNA extracted from yeast strain PLY22 (Table 1) was analyzed by Northern blotting using the following uniformly labeled DNA probes: 2305 bp from the coding region of UPF1; 652 bp from the coding region of *SUP14* (encoding ribosomal protein S3); 1097 bp from the coding region of *TCM1* (encoding ribosomal protein L3). The G+C content of each probe is 39.5, 44, and 43.8%, respectively.

[b]Ratios were calculated using the adjusted CPM detected for each DNA/RNA hybrid. Each ratio represents the average value for four experiments. The standard deviation is shown in parentheses. The adjusted CPM was calculated using the formula (absolute CPM [minus] background)/probe length in kb). In each case the CPM detected above background using the Betascope blot analyzer corresponds to visible bands detected by autoradiography of the Northern blots. The limit of sensitivity for detection of radioactivity by the Betascope in these experiments was calculated to be 0.5 CPM above background (for five standard deviations).

cytoplasmic (Leeds *et al.*, 1992). Furthermore, the nonsense mRNA decay pathway is triggered by premature translational termination, suggesting that translation, which is primarily a cytoplasmic event, plays a role in decay.

A nuclear location either for UPF1 or the decay pathway itself was also considered possible. UPF1 could influence the rate of nonsense mRNA decay indirectly by affecting ribosome structure from a location in the nucleolus where ribosomal subunits are assembled. Furthermore, recent studies in mammals have led to the suggestion that nonsense mRNA decay may be initiated by translation of nonsense mRNAs that are still in the process of being transported from the nucleus to the cytoplasm (Belgrader *et al.*, 1993, 1994; Cheng and Maquat, 1993).

A role for UPF1 in the mitochondrion was suggested by results showing that over-expression of UPF1 from a multi-copy plasmid suppresses a mitochondrial mRNA splicing defect (Ben Asher *et al.*, 1989; Altamura *et al.*, 1992). Also, loss of UPF1 function confers a reduced rate of growth in medium containing lactate as a sole carbon source, suggesting a requirement for UPF1 in respiratory processes that occur in the mitochondria.

To find out where UPF1 is located, we placed a DNA fragment coding for three copies of an influenza HA epitope in frame at the 3′ end of the *UPF1* ORF. Detection of the tagged product UPF1–3EP was achieved using commercially available 12CA5 monoclonal antibodies. We had previously found that a single copy of the same epitope placed at the same position in UPF1 provided an insufficient signal. It was visible on Western blots only when the singly-tagged protein was overproduced. We also found an unacceptable level of cross-reaction with an endogenous yeast protein that has an apparent molecular weight of 51 k both by Western blotting and by immunofluorescent microscopy.

All of the problems with the single-epitope tagging system were avoided using the triple-epitope. UPF1–3EP was detected in protein extracts from a strain carrying one copy of UPF1–3EP on a centromeric plasmid. No significant cross-reaction was evident by Western blotting, immunofluorescent microscopy, or confocal microscopy. Furthermore, tagging the C-terminus provided another advantage by minimizing the chance of detecting incomplete, nascent UPF1–3EP polypeptides on polyribosomes. Nascent UPF1–3EP is released from polyribosomes soon after synthesis of the C-terminal epitopes. Any epitopes detected in association with polyribosomes are therefore likely to be located on full length UPF1–3EP protein molecules that have re-associated with polyribosomes.

The validity of our results depends on whether UPF1–3EP retains its function despite the addition of 37 amino acids to the C-terminus. We assayed UPF1–3EP function in strains lacking the normal UPF1 protein using three criteria: (1) the ability to suppress growth in an allo-frameshift suppression assay (Figure 1; Culbertson *et al.*, 1980), (2) the ability to restore growth in medium containing lactate as the sole carbon source (Figure 4; Altamura *et al.*, 1992) and, (3) the ability to reduce steady-state accumulation of *his4–38* mRNA through accelerated decay (Leeds *et al.*, 1991). Our results show that UPF1–3EP is 86% (± 5%) as efficient as the wild-type UPF1 protein in promoting nonsense mRNA decay. This modest reduction in function is recessive. Because UPF1–3EP is functional, we assume that its cellular location is identical to wild-type UPF1.

Our results indicate that all of the detectable UPF1–3EP is found in the cytoplasm. We could not detect any UPF-3EP in the nucleus using three different approaches. UPF1-specific fluorescent antibody staining was absent in the region of the nucleus that stains with DAPI. Little overlap in differential fluorescent staining was detected when cells were double labeled with fluorescent antibodies that recognize UPF1–3EP and SEN1::βgal fusion protein that is distributed exclusively in the nucleoplasm. Finally, in cells double labeled with antibodies that recognize UPF1–3EP and the ER protein KAR2, no UPF1–3EP–specific fluorescence was observed inside the boundary of the nuclear envelope that is outlined by KAR2 staining in 80% of cells. Considering the strength of the cytoplasmic fluorescent signal ob-

served using the triple epitope tag, the evidence favors the view that the vast majority of UPF1–3EP is in the cytoplasm. Nonetheless, there could be a minor fraction of nuclear or nucleolar UPF1–3EP that is present at a concentration below the detection limits or that is refractory to antibody staining.

Cytochemical studies comparing the location of UPF1–3EP with the mitochondrial protein MAS2 suggest that there is little overlap in the distribution of these two proteins. The possible presence of some UPF1–3EP in the mitochondrion was further tested using a cellular fractionation procedure that separates mitochondria from other cellular components. A small amount of UPF1–3EP was detected in the mitochondrial fraction, but it was proteinase K sensitive and therefore located outside the mitochondria. The effects of UPF1 on mitochondrial mRNA splicing, which takes place inside the organelle, is therefore likely to be an indirect consequence of UPF1 function. UPF1 may affect the level of expression of a yet to be identified nuclear gene whose product is required for mitochondrial function. This view is plausible because it has already been shown that UPF1 affects the expression of some natural mRNAs (Leeds *et al.*, 1991).

UPF1 Associates with Polyribosomes

We assessed the potential association of UPF1 with polyribosomes by examining the behavior of UPF1–3EP and ribosomal protein L1 in sucrose gradients. The distribution of both proteins exhibited similar changes using three different sets of conditions that alter the polyribosome profile. When cycloheximide was omitted, about 20% of both UPF1–3EP and L1 shifted out of fractions containing polyribosomes and into fractions containing 80S ribosomal particles. When preparations were treated with RNase A, 65–85% of both UPF1–3EP and L1 shifted from the polyribosomes to the fractions containing 80S ribosomal particles. Finally, when cells were shifted from a synthetic to a rich medium that supports more rapid growth, 20–30% of both UPF1–3EP and L1 shifted into fractions containing polyribosomes. UPF1–3EP and L1 may exhibit a similar shift due to an association of UPF1 with polyribosomes. Further experiments will be required to establish the molecular basis of the proposed association.

A variable proportion of UPF1–3EP was detected in fractions that do not contain ribosomal subunits, 80S ribosomal particles, or polyribosomes. In the presence of 50 μg/ml cycloheximide, about 20% of UPF1–3EP was found in fractions containing monomers, small aggregates, or small complexes. Less than 1% was found in these fractions when cycloheximide was omitted. RNase A treatment in the presence or absence of cycloheximide also caused up to 50% of UPF1–3EP to shift from the polyribosome fractions to the ribosome-free fractions. Combined with the observation that complete loss of UPF1 function confers cycloheximide hypersensitivity (Leeds *et al.*, 1992), we are considering the possibility that cycloheximide may inhibit the association of UPF1–3EP with polyribosomes either indirectly or by direct competition for a binding site on the 60S ribosomal subunit.

Yeast translational initiation factors, such as GCN2 (Ramirez *et al.*, 1991), behave in sucrose gradients as though they interact with ribosomes during translational initiation. GCN2 preferentially associates with 60S ribosomal subunits, 80S ribosomal particles, and polyribosomes during exponential growth and it cosediments with 40S and 60S ribosomal subunits when polyribosomes are disaggregated. These results suggest that GCN2 interacts with ribosomes during the translation initiation cycle (Ramirez *et al.*, 1991). By contrast, UPF1 may associate with polyribosomes after formation of an initiation complex. UPF1–3EP accumulates in fractions containing 80S ribosomal particles and polyribosomes, but not in fractions containing the 40S and 60S ribosomal subunits during exponential growth. When polyribosomes are disaggregated, UPF1–3EP co-sediments with 80S ribosomal particles, but does not appear to accumulate in fractions containing 40S or 60S ribosomal subunits. UPF1–3EP therefore behaves more like a translational elongation or termination factor.

Like other known translation factors that utilize GTP hydrolysis to dissociate from polyribosomes, UPF1 contains a consensus motif for GTP binding that has the potential to control cyclic binding and release of UPF1 from polyribosomes. It is generally thought that conformational differences between GDP- and GTP-bound forms of the translation factors influence the relative rates of association and dissociation of the factors from ribosomes. However, even if UPF1 binds GTP for a similar purpose, it differs from other known G-proteins that function in translation in that it is not required to support normal cell growth and therefore does not perform a function in protein synthesis that is essential for growth (Leeds *et al.*, 1991).

Functional Relationships between UPF1, Polyribosomes, and Nonsense mRNA Decay

Although UPF1 function has been shown to be required in order for nonsense mRNA decay to occur, it has not yet been established that it plays a direct role in the decay pathway. Genetic evidence suggesting that a direct role is possible comes primarily from the analysis of both recessive and dominant mutations in *UPF1*.

Leeds *et al.* (1992) reported that the phenotypes of dominant point mutations in *UPF1* resemble the phenotype of a recessive gene disruption that confers complete loss of function. Both types of alleles result

in the stabilization of nonsense mRNAs. The strength of the dominant phenotype was found to depend on the dosage of the dominant allele relative to the wild-type allele (Leeds *et al.*, 1992). Nonsense mRNA decay was inhibited to a greater extent when a dominant allele was over-expressed relative to the wild-type allele. Dominant UPF1 mutations meet all of the criteria of the classical dominant-negative phenotype. A dominant-negative UPF1 protein might interfere with wild-type UPF1 function by one of two general mechanisms (Herskowitz, 1987). It could act as a poison subunit by forming a nonfunctional multimer with wild-type UPF1 or with other proteins that interact with UPF1. Alternatively, it could bind a substrate of UPF1 more tightly than wild type and block UPF1 function by preventing access to a substrate.

Dominant-negative UPF1 mutations map exclusively within a conserved sequence motif (Leeds *et al.*, 1992) that shares similarity with proteins that have helicase and/or RNA-dependent NTPase activity (Koonin, 1993). The identification of dominant-negative mutations exclusively in this region suggests the presence of a functional domain in UPF1 that has the potential to interact with RNA, and that this interaction is important in the underlying mechanism for the dominant-negative phenotype. The identity of the proposed RNA could provide a way to determine whether UPF1 performs a catalytic function in the nonsense mRNA decay pathway.

In the absence of more direct information regarding UPF1 function, we cannot definitively infer whether it associates with polyribosomes for the purpose of catalyzing a step in the nonsense mRNA decay pathway or whether it associates with polyribosomes to perform a function in translation that indirectly promotes nonsense mRNA decay. What is known is that the mRNA substrate for decay as well as UPF1, a potential catalyst of a step in the decay pathway, are both associated with polyribosomes (Leeds *et al.*, 1991). Given the uncertainty regarding UPF1 function, our finding that UPF1 is primarily cytoplasmic may not necessarily mean that nonsense mRNA decay is a cytoplasmic event. It remains possible that this type of decay occurs at the interface of the nucleus and cytoplasm as proposed by Belgrader *et al.* (1994).

Northern blotting was used as an indirect way to measure the relative abundance of UPF1 to ribosomes. After controlling as much as possible for differences in hybridization efficiency, we found that ribosomal protein S3 and L3 mRNA accumulation was about 100-fold lower. Furthermore, the codon bias index of 0.21 for UPF1 (Leeds *et al.*, 1992) is typical of genes expressed at a low level, whereas the codon bias indices for S3 and L3 (0.93 and 0.88, respectively) are typical of yeast genes expressed at a high level (Bennetzen and Hall, 1982). Even assuming that the rates of translation of the three genes are similar, the possibility of 1:1 ratio of UPF1 to ribosomes seems unlikely. The evidence to date suggests that there are far fewer UPF1 molecules than ribosomes per cell.

If UPF1 associates with polyribosomes to promote nonsense mRNA decay, it remains to be explained how those polyribosomes containing target mRNAs could be identified by UPF1 fast enough to affect the decay rate given the apparent low abundance of UPF1 relative to ribosomes. Some target mRNAs, such as *his4–38* mRNA, have a half-life of 3–4 min (Leeds *et al.*, 1991), which indicates that the time interval may be too short for a relatively small number of UPF1 protein molecules to randomly scan polyribosomes for the presence of target mRNAs. This raises two possibilities. Polyribosomes or target mRNAs may be tagged in some way that allows for selective recognition, similar in principle to the way that proteins are tagged for degradation by ubiquitin. Alternatively, UPF1 may act downstream in the decay pathway and might require the presence of other, perhaps more abundant, proteins that associate with polyribosomes or target mRNAs first. Experiments designed to distinguish between these alternatives are currently in progress.

ACKNOWLEDGMENTS

This research was supported by the College of Agricultural and Life Sciences, University of Wisconsin (Madison, WI), United States Public Health Service grant GM-26217 (M.R.C.), Alberta Heritage Foundation for Medical Research supplemental research allowance, and Natural Sciences and Engineering Research Council of Canada postdoctoral fellowship (A.L.A.). This is paper no. 3392 of the University of Wisconsin Laboratory of Genetics. We are grateful to S. Paddock for technical assistance in confocal microscopy, T. Hook for help with the fractionation experiments, R. Castaldo for technical advice, and L. Olds for preparation of the figures. We would like to thank M. Rose, H.M. Fried, D. Ursic, and J. Hendrick for plasmids, and S. Blair, M. Rose, J. Woolford, B. Craig, A. Hopper, and G. Schatz for antibodies used in these studies. We thank J. Ross for critical reading of the manuscript.

REFERENCES

Altamura, N., Dujardin, G., Groudinsky, O., and Slonimski, P.P. (1994). Two adjacent nuclear genes, *ISF1* and *NAM7/UPF1*, cooperatively participate in mitochondrial functions in *Saccharomyces cerevisiae*. Mol. Gen. Genet. *242*, 49–56.

Altamura, N., Groudinsky, O., Dujardin, G., and Slonimski, P.P. (1992). *NAM7* nuclear gene encodes a novel member of a family of helicases with a Zn-ligand motif and is involved in mitochondrial functions in *Saccharomyces cerevisiae*. J. Mol. Biol. *224*, 575–587.

Ausubel, F.M., Brent, R., Kingston, R.E., Moore, D.D., Seideman, J.G., Smith, J.A., and Struhl, K. (ed.) (1993). Current Protocols in Molecular Biology, New York: Green Publishing Associates and Wiley-Interscience.

Belgrader, P., Cheng, J., and Maquat, L.E. (1993). Evidence to implicate translation by ribosomes in the mechanism by which nonsense codons reduce the nuclear level of human triosephosphate isomerase mRNA. Proc. Natl. Acad. Sci. USA *90*, 482–486.

Belgrader, P., Cheng, J., Zhou, X., Stephenson, L.S., and Maquat, L.E. (1994). Mammalian nonsense codons can be *cis* effectors of nuclear mRNA half-life. Mol. Cell. Biol. *14*, 8219–8228.

Ben Asher, E.B., Groudinsky, O., Dujardin, G., Altamura, N., Kermorgant, M., and Slonimski, P.P. (1989). Novel class of nuclear genes involved in both mRNA splicing and protein synthesis in *Saccharomyces cerevisiae* mitochondria. Mol. Gen. Genet. *215*, 517–528.

Bennetzen, J.L., and Hall, B.D. (1982). Codon selection in yeast. J. Biol. Chem. *257*, 3026–3031.

Birnboim, H.C., and Doly, J. (1979). A rapid alkaline extraction procedure for screening recombinant plasmid DNA. Nucleic Acids Res. *7*, 1513–1523.

Bollag, D.M., and Edelstein, S.J. (1991). Protein Methods, New York: Wiley-Liss, Inc.

Cheng, J., Fogel-Petrovic, M., and Maquat, L.E. (1990). Translation to near the distal end of the penultimate exon is required for normal levels of spliced triosephosphate isomerase mRNA. Mol. Cell. Biol. *10*, 5215–5225.

Cheng, J., and Maquat, L.E. (1993). Nonsense codons can reduce the abundance of nuclear mRNA without affecting the abundance of pre-mRNA or the half-life of cytoplasmic mRNA. Mol. Cell. Biol. *13*, 1892–1902.

Culbertson, M.R., Underbrink, K.M., and Fink, G.R. (1980). Frameshift suppression in *Saccharomyces cerevisiae*. II. Genetic properties of group II suppressors. Genetics *95*, 833–853.

DeMarini, J.D., Winey, M., Ursic, D., Webb, F., and Culbertson, M.R. (1992). SEN1, a positive effector of tRNA-splicing endonuclease in *Saccharomyces cerevisiae*. Mol. Cell. Biol. *12*, 2154–2164.

Deshmukh, M., Tsay, Y.-F., Paulovich, A.G., and Woolford, J.L., Jr. (1993). Yeast ribosomal protein L1 is required for the stability of newly synthesized 5S rRNA and the assembly of 60S ribosomal subunits. Mol. Cell. Biol. *13*, 2835–2845.

Donahue, T.F., Farabaugh, P.J., and Fink, G.R. (1981). Suppressible glycine and proline four base codons. Science *212*, 455–457.

Feinberg, A.P., and Vogelstein, B. (1983). A technique for radiolabelling DNA restriction endonuclease fragments to high specific activity. Anal. Biochem. *132*, 6–13.

Fried, H.M., and Warner, J.R. (1981). Cloning of yeast gene for trichodermin resistance and ribosomal protein L3. Proc. Natl. Acad. Sci. USA *78*, 238–242.

Gaber, R.F., and Culbertson, M.R. (1982). Frameshift suppression in *Saccharomyces cerevisiae*. IV. New suppressors among spontaneous co-revertants of the group-II *his4–206* and *leu2–3* frameshift mutations. Genetics *101*, 345–367.

Gozalbo, D., and Holmann, S. (1990). Nonsense suppressors partially revert the decrease of the mRNA level of a nonsense mutant allele in yeast. Curr. Genet. *17*, 77–79.

Grant, P., Sanchez, L., and Jimenez, A. (1974). Crytopleurine resistance: genetic locus for a 40S ribosomal component in *Saccharomyces cerevisiae*. J. Bacteriol. *120*, 1308–1314.

He, F., Peltz, S.W., Donahue, J.L., Rosbash, M., and Jacobson, A. (1993). Stabilization and ribosome association of unspliced pre-mRNAs in a yeast *upf1*$^-$ mutant. Proc. Natl. Acad. Sci. USA *90*, 7034–7038.

Herbert, C.J., Labouesse, M., Dujardin, G., and Slonimski, P.P. (1988). The NAM2 proteins from *S. cerevisiae* and *S. douglasii* are mitochondrial leucyl-tRNA synthetases, and are involved in mRNA splicing. EMBO J. *7*, 473–483.

Herskowitz, I. (1987). Functional inactivation of genes by dominant negative mutations. Nature *329*, 219–222.

Ito, H., Fukuda, Y., Murata, K., and Kimura, A. (1983). Transformation of intact yeast cells treated with alkali cations. J. Bacteriol. *153*, 163–168.

Jensen, R.E., and Yaffe, M.P. (1988). Import of proteins into yeast mitochondria: the nuclear *MAS2* gene encodes a component of the processing protease that is homologous to the *MAS1*-encoded subunit. EMBO J. *7*, 3863–3871.

Klessig, D.F., and Berry, J.O. (1983). Improved filter hybridization method for detection of single copy sequences in large eukaryotic genomes. Plant Mol. Biol. Rep. *1*, 12–18.

Koonin, E.V. (1993). A new group of putative RNA helicases. Trends Biochem. Sci. *17*, 495–497.

Leeds, P., Peltz, S.W., Jacobson, A., and Culbertson, M.R. (1991). The product of the yeast *UPF1* gene is required for rapid turnover of mRNAs containing a premature translational termination codon. Genes Dev. *5*, 2303–2314.

Leeds, P., Wood, J.M., Lee, B.-S., and Culbertson, M.R. (1992). Gene products that promote mRNA turnover in *Saccharomyces cerevisiae*. Mol. Cell. Biol. *12*, 2165–2177.

Losson, R., and Lacroute, F. (1979). Interference of nonsense mutations with eukaryotic messenger RNA stability. Proc. Natl. Acad. Sci. USA *76*, 5134–5137.

Mendenhall, M.D., Leeds, P., Fen, H., Mathison, L., Zwick, M., Sleiziz, C., and Culbertson, M.R. (1987). Frameshift suppressor mutations affecting the major glycine transfer RNAs of *Saccharomyces cerevisiae*. J. Mol. Biol. *194*, 41–58.

Peltz, S.W., and Jacobson, A. (1993). mRNA turnover in *Saccharomyces cerevisiae*. In: Control of Messenger RNA Stability, ed. G. Brawerman and J. Belasco, San Diego, CA: Academic Press Inc., 291–327.

Pulak, R., and Anderson, P. (1993). mRNA surveillance by the *Caenorhabditis elegans smg* genes. Genes Dev. *7*, 1885–1897.

Ramirez, M., Wek, R.C., and Hinnenbush, A.G. (1991). Ribosome association of GCN2 protein kinase, a translational activator of the *GCN4* gene of *Saccharomyces cerevisiae*. Mol. Cell. Biol. *11*, 3027–3036.

Roof, D.M., Meluh, P.B., and Rose, M.D. (1992). Kinesin-related proteins required for assembly of the mitotic spindle. J. Cell Biol. *118*, 95–108.

Rose, M.D., Misra, L.M., and Vogel, J.P. (1989). KAR2, a karyogamy gene, is the yeast homolog of the mammalian BiP/GRP78 gene. Cell *57*, 1211–1221.

Rose, M.D., Winston, F., and Hieter, P. (1990). Methods in Yeast Genetics, Cold Spring Harbor, NY: Cold Spring Harbor Laboratory Press.

Sachs, A.B. (1993). Messenger RNA degradation in eukaryotes. Cell *74*, 413–421.

Sachs, A.B., and Davis, R.W. (1989). The poly(A) binding protein is required for poly(A) shortening and 60S ribosomal subunit-dependent translational initiation. Cell *58*, 857–867.

Sambrook, J., Fritsch, E.F., and Maniatis, T. (1989). Molecular Cloning: A Laboratory Manual, Cold Spring, NY: Cold Spring Harbor Laboratory Press.

Sanger, F., Nicklen, S., and Coulson, A.R. (1977). DNA sequencing with chain-terminating inhibitors. Proc. Natl. Acad. Sci. USA *74*, 5463–5467.

Sikorski, R.S., and Hieter, P. (1989). A system of shuttle vectors and yeast host strains designed for efficient manipulation of DNA in *Saccharomyces cerevisiae*. Genetics *122*, 19–27.

Woolford, J.L., Jr., and Warner, J.R. (1991). The ribosome and its synthesis. In: The Molecular and Cellular Biology of the Yeast *Saccharomyces*: Genome Dynamics, Protein Synthesis and Energetics, vol. 1, ed. J.R. Broach, J.R. Pringle, and E.W. Jones, Cold Spring Harbor, NY: Cold Spring Harbor Laboratory Press, 587–626.